

Reactions of the Electron-Rich Triply Bonded Dirhenium(II) Complexes $\text{Re}_2\text{X}_4(\mu\text{-dppm})_2$ ($\text{X} = \text{Cl}, \text{Br}$) with Dioxygen. 1. Multielectron Redox Chemistry with Preservation of the $\text{Re}_2\text{X}_4(\text{dppm})_2$ Unit

Stuart L. Bartley,¹ Kim R. Dunbar,¹ Keng-Yu Shih,² Phillip E. Fanwick,² and Richard A. Walton^{*,2}

Departments of Chemistry, Michigan State University, East Lansing, Michigan 48824, and Purdue University, West Lafayette, Indiana 47907-1393

Received November 6, 1992

The dirhenium(II) complexes $\text{Re}_2\text{X}_4(\mu\text{-dppm})_2$ (**1a**, $\text{X} = \text{Cl}$; **1b**, $\text{X} = \text{Br}$; $\text{dppm} = \text{Ph}_2\text{PCH}_2\text{PPh}_2$), which contain an electron-rich Re–Re triple bond, react with dioxygen in a variety of solvents to afford $\text{Re}_2(\mu\text{-O})(\mu\text{-X})(\text{O})\text{X}_3(\mu\text{-dppm})_2$ (**2a**, $\text{X} = \text{Cl}$; **2b**, $\text{X} = \text{Br}$) and $\text{Re}_2(\mu\text{-O})(\text{O})_2\text{X}_4(\mu\text{-dppm})_2$ (**3a**, $\text{X} = \text{Cl}$; **3b**, $\text{X} = \text{Br}$) in which the $\text{Re}_2\text{X}_4(\mu\text{-dppm})_2$ entity is preserved and net 4- and 6-electron oxidations of the dirhenium unit have occurred. The complexes of type **2**, which are weakly paramagnetic and possess Knight-shifted NMR spectra, have edge-sharing bioctahedral structures as shown by a single-crystal X-ray structure determination on a crystal of composition $\text{Re}_2(\mu\text{-O})(\mu\text{-Cl})(\text{O})\text{Cl}_3(\mu\text{-dppm})_2 \cdot (\text{CH}_3)_2\text{CO}$ (**2a**· $(\text{CH}_3)_2\text{CO}$). The structure solution was complicated by a disorder involving the terminal oxo ligand and the syn terminal chloro ligand on the adjacent Re atom. The Re...Re distance is very long (3.363(2) Å). Crystal data for **2a**· $(\text{CH}_3)_2\text{CO}$ (+23 °C): triclinic space group $P\bar{1}$ (No. 2), $a = 16.069(6)$ Å, $b = 16.540(5)$ Å, $c = 12.214(2)$ Å, $\alpha = 109.18(2)^\circ$, $\beta = 99.09(3)^\circ$, $\gamma = 101.01(3)^\circ$, $V = 2923(2)$ Å³, and $Z = 2$. The structure was refined to $R = 0.068$ ($R_w = 0.082$) for 6553 data with $I > 3.0\sigma(I)$. Complex **2a** can be derivatized by reaction with isocyanide ligands (RNC ; $\text{R} = \text{C}_6\text{H}_3\text{-2,6-Me}_2$ (xylyl), CHMe_2 , CMe_3 , C_6H_{11}) and acetonitrile to give complexes of the type $\text{Re}_2(\mu\text{-O})(\text{O})\text{Cl}_4(\mu\text{-dppm})_2(\text{L})$ (**4**, $\text{L} = \text{RNC}$; **5**, $\text{L} = \text{MeCN}$) which like **2a** are weakly paramagnetic and have Knight-shifted NMR spectra. The structure of crystals of composition $\text{Re}_2(\mu\text{-O})(\text{O})\text{Cl}_4(\mu\text{-dppm})_2(\text{CN}^{\text{xylyl}}) \cdot \text{CH}_2\text{Cl}_2 \cdot \text{H}_2\text{O}$ (**4a**) has been established by X-ray crystallography. The structure is an unsymmetrical corner-sharing bioctahedral $\text{Cl}_3\text{Re}(\mu\text{-O})(\mu\text{-dppm})_2\text{Re}(\text{O})\text{Cl}(\text{CN}^{\text{xylyl}})$, in which the rhenium centers can formally be represented as $\text{Re}(\text{III})\text{-Re}(\text{V})$, i.e. $\text{Re}^{\text{III}}\cdots\text{O}=\text{Re}^{\text{V}}=\text{O}$. Crystal data for **4a** (+20 °C): triclinic space group $P\bar{1}$ (No. 2), $a = 14.316(3)$ Å, $b = 14.818(2)$ Å, $c = 16.840(2)$ Å, $\alpha = 99.60(1)^\circ$, $\beta = 106.38(1)^\circ$, $\gamma = 97.26(1)^\circ$, $V = 3322(2)$ Å³, and $Z = 2$. The structure was refined to $R = 0.056$ ($R_w = 0.082$) for 5978 data with $I > 3.0\sigma(I)$. The compounds of type **4** have been oxidized by $[(\eta^5\text{-C}_5\text{H}_5)_2\text{Fe}]\text{PF}_6$ to afford the mixed-valence paramagnetic complexes $[\text{Re}_2(\mu\text{-O})(\text{O})\text{Cl}_4(\mu\text{-dppm})(\text{CNR})]\text{PF}_6$ (**6**; $\text{R} = \text{C}_6\text{H}_3\text{-2,6-Me}_2$, CHMe_2 , CMe_3). The dirhenium(V) complexes $\text{Re}_2(\mu\text{-O})(\text{O})_2\text{X}_4(\mu\text{-dppm})_2$ (**3**), which are the final products of the oxygenation of **1** and **2**, have a centrosymmetric corner-sharing bioctahedral structure. The structures of two different crystals of **3a** ($\text{X} = \text{Cl}$), which contain either two molecules of lattice acetone (**3a**· $(\text{CH}_3)_2\text{CO}$) or two molecules of dichloromethane (**3a**· CH_2Cl_2), have been determined. Crystal data for **3a**· $(\text{CH}_3)_2\text{CO}$ (+23 °C): triclinic space group $P\bar{1}$ (No. 2), $a = 11.193(2)$ Å, $b = 12.882(2)$ Å, $c = 10.892(2)$ Å, $\alpha = 101.95(1)^\circ$, $\beta = 113.30(1)^\circ$, $\gamma = 75.52(1)^\circ$, $V = 1386.3(4)$ Å³, and $Z = 1$. The structure was refined to $R = 0.029$ ($R_w = 0.058$) for 4209 data with $I > 3.0\sigma(I)$. Crystal data for **3a**· CH_2Cl_2 (+20 °C): triclinic space group $P\bar{1}$ (No. 2), $a = 11.264(4)$ Å, $b = 11.317(4)$ Å, $c = 12.966(7)$ Å, $\alpha = 103.86(4)^\circ$, $\beta = 104.24(4)^\circ$, $\gamma = 113.54(3)^\circ$, $V = 1358(3)$ Å³, and $Z = 1$. The structure was refined to $R = 0.052$ ($R_w = 0.072$) for 3538 data with $I > 3.0\sigma(I)$.

Introduction

The dirhenium(II) complexes $\text{Re}_2\text{X}_4(\mu\text{-dppm})_2$ (**1a**, $\text{X} = \text{Cl}$; **1b**, $\text{X} = \text{Br}$), where $\text{dppm} = \text{Ph}_2\text{PCH}_2\text{PPh}_2$,^{3,4} are extremely useful reagents⁵ in dirhenium chemistry because of the facility with which they are oxidized to higher valent species. These compounds, which possess the electron-rich triply-bonded ground-state configuration $\sigma^2\pi^4\delta^2\delta^{*2}$, can be utilized in the reductive coupling of organic molecules,^{6,7} in oxidative addition reactions across the $\text{Re}\equiv\text{Re}$ bond,⁸⁻¹⁰ and in the formation of charge-transfer complexes.¹¹

Although **1a** and **1b** can be handled in the air for short periods without significant levels of degradation, we have noticed during the course of many previous studies that a relatively slow reaction of the solid complexes with O_2 does occur and that its rate is enhanced in solutions of these complexes in a variety of solvents. We now describe details of the reactions of **1** with O_2 in which net 4- and 6-electron redox reactions have been found to occur with formation of the compounds $\text{Re}_2(\mu\text{-O})(\mu\text{-X})(\text{O})\text{X}_3(\mu\text{-dppm})_2$ (**2**) and $\text{Re}_2(\mu\text{-O})(\text{O})_2\text{X}_4(\mu\text{-dppm})_2$ (**3**). This behavior is very unusual in the field of dimetal multiple bond chemistry^{12,13} because these oxygenation reactions proceed without loss of any of the ligands from the precursor complex.¹⁴

(1) Michigan State University.

(2) Purdue University.

(3) Barder, T. J.; Cotton, F. A.; Dunbar, K. R.; Powell, G. L.; Schwotzer, W.; Walton, R. A. *Inorg. Chem.* **1985**, *24*, 2550.

(4) Cutler, A. R.; Derringer, D. R.; Fanwick, P. E.; Walton, R. A. *J. Am. Chem. Soc.* **1988**, *110*, 5024.

(5) Walton, R. A. *Polyhedron* **1989**, *8*, 1689.

(6) Esjornson, D.; Derringer, D. R.; Fanwick, P. E.; Walton, R. A. *Inorg. Chem.* **1989**, *28*, 2821.

(7) Shih, K.-Y.; Fanwick, P. E.; Walton, R. A. Unpublished results.

(8) Qi, J.-S.; Schrier, P. W.; Fanwick, P. E.; Walton, R. A. *Inorg. Chem.* **1992**, *31*, 258.

(9) Shih, K.-Y.; Fanwick, P. E.; Walton, R. A. *J. Chem. Soc., Chem. Commun.* **1992**, 375.

(10) (a) Ara, I.; Fanwick, P. E.; Walton, R. A. *Polyhedron* **1992**, *11*, 1277. (b) Ara, I.; Fanwick, P. E.; Walton, R. A. *J. Cluster Sci.* **1992**, *3*, 83.

(11) Bartley, S. L.; Dunbar, K. R. *Angew. Chem., Int. Ed. Engl.* **1991**, *30*, 448.

(12) Cotton, F. A.; Walton, R. A. *Multiple Bonds Between Metal Atoms*, 2nd ed.; Oxford University Press: Oxford, U.K., 1993.

(13) Cotton, F. A.; Walton, R. A. *Struct. Bonding (Berlin)* **1985**, *62*, 1.

(14) Some of these results have been described in a preliminary communication; see: Bartley, S. L.; Dunbar, K. R.; Shih, K.-Y.; Fanwick, P. E.; Walton, R. A. *J. Chem. Soc., Chem. Commun.* **1993**, 98.

Experimental Section

Starting Materials and Reaction Procedures. The dirhenium complexes $\text{Re}_2\text{X}_4(\text{dppm})_2$ (**1a**, X = Cl; **1b**, X = Br) were prepared as described in the literature.^{3,4} In studies carried out at MSU all solvents were predried over 4-Å molecular sieves. Benzene, toluene, diethyl ether, and THF were distilled from sodium/potassium benzophenone ketyl radical. Dichloromethane was distilled under a nitrogen atmosphere from P_2O_5 . Acetone was distilled under a nitrogen atmosphere from 3-Å molecular sieves. Less rigorous drying procedures were used at PU, thereby providing a means of detecting the influence (if any) of differing small amounts of water upon the course of reactions described in this report. As far as we could ascertain, similar results were obtained at the two locations. Reactions were performed with the use of standard Schlenk line techniques.

A. Synthesis of $\text{Re}_2(\mu\text{-O})(\mu\text{-X})(\text{O})\text{X}_3(\mu\text{-dppm})_2$ (X = Cl, Br). (i) X = Cl (**2a**). A mixture of $\text{Re}_2\text{Cl}_4(\text{dppm})_2$ (**1a**) (0.10 g, 0.078 mmol) and 2 mL of CHCl_3 was stirred under an atmosphere of air for 7 h. The brown solid was filtered off, washed with diethyl ether (2 × 5 mL), and vacuum dried; yield 0.068 g (66%). Anal. Calcd for $\text{C}_{50}\text{H}_{44}\text{Cl}_4\text{O}_2\text{P}_4\text{Re}_2$: C, 45.66; H, 3.38; Cl, 10.78. Found: C, 45.09; H, 3.18; Cl, 10.55. The filtrate was evaporated to dryness, and 3 mL of THF was added to the brown residue. This mixture was stirred in the air at room temperature for 5 h. The resulting green solid was filtered off, washed with 5 mL of diethyl ether, and vacuum dried; yield 0.023 g (22%). The spectroscopic and electrochemical properties of this product showed it to be the complex **3a** (see section B(i)).

With reaction conditions very similar to those described above, **2a** can be prepared with the use of acetone, benzene, or toluene as the reaction solvent. When THF was used as the solvent, this product was always admixed with **3a** (see section B(i)).

A modification of this procedure involved the use of O_2 instead of air. In a typical reaction, a solution of **1a** (0.100 g, 0.078 mmol) in acetone (20 mL) was purged with O_2 gas for 2 h. During this period, the solution color changed from purple to wine-red with deposition of a brown microcrystalline solid. The mixture was allowed to stand undisturbed for 12 h during which time the solution color changed to yellow-brown. The resulting brown precipitate was collected by filtration, washed with acetone (3 × 5 mL), and vacuum dried; yield 0.071 g (69%). Anal. Calcd for $\text{C}_{50}\text{H}_{44}\text{Cl}_4\text{O}_2\text{P}_4\text{Re}_2$: C, 45.66; H, 3.38. Found: C, 46.21; H, 3.39. When the filtrate was set aside and allowed to evaporate slowly, a small quantity of the green crystalline complex **3a** was obtained as its bis(acetone) solvate $\text{Re}_2(\mu\text{-O})(\text{O})_2\text{Cl}_4(\mu\text{-dppm})_2 \cdot 2(\text{CH}_3)_2\text{CO}$ (see section B(ii)).

Results identical to these were obtained upon the reaction **1a** with O_2 in benzene or toluene. Similar behavior was observed when CH_2Cl_2 was used as the reaction solvent, but in this instance the sample of **2a** was isolated after a reaction time of 2 h by treating the wine-red reaction solution with diethyl ether (20 mL), filtering, and washing the insoluble product with acetone (3 × 5 mL), and vacuum drying; yield 95%.

(ii) X = Br (**2b**). A sample of this complex was prepared from $\text{Re}_2\text{Br}_4(\mu\text{-dppm})_2$ (**1b**) (0.100 g, 0.68 mmol) through the use of a procedure similar to that described for the preparation of the analogous chloride complex (**2a**); yield 0.062 g (61%). The identity of this product was established from a comparison of its spectroscopic and electrochemical properties with those of **2a**.

B. Synthesis of $\text{Re}_2(\mu\text{-O})(\text{O})_2\text{X}_4(\mu\text{-dppm})_2$ (X = Cl, Br). (i) X = Cl (**3a**). (a) From $\text{Re}_2\text{Cl}_4(\mu\text{-dppm})_2$. A quantity of **1a** (0.050 g; 0.039 mmol) was dissolved in 4 mL of O_2 -saturated THF and the mixture stirred at room temperature. The initial purple colored solution slowly changed to brown then to green, whereupon a green solid deposited in the flask over a period of 10 h. The green product was filtered off, washed with diethyl ether (2 × 5 mL), and vacuum dried; yield 0.039 g (74%). Anal. Calcd for $\text{C}_{50}\text{H}_{44}\text{Cl}_4\text{O}_3\text{P}_4\text{Re}_2$: C, 45.11; H, 3.34. Found: C, 44.68; H, 3.18. The product can be purified further by recrystallization from CH_2Cl_2 -diethyl ether mixtures.

In a separate experiment a Schlenk-tube containing **1a** (0.100 g, 0.078 mmol) in CH_2Cl_2 (20 mL) was purged with O_2 gas for 1.5 h to give an opaque wine-red solution. The solution was set aside whereupon it slowly transformed to a deep olive-green color over a 4-day period. The solution volume was reduced to ca. 5 mL and then treated with 20 mL of acetone. Within 12 h, a mixture of block-shaped green crystals and feathery green crystals had formed. The feathery crystals slowly redissolved within 3 days. The crop of large green crystals was filtered from the yellow-brown filtrate, washed with a minimal amount of cold acetone, and vacuum dried; yield 0.05 g (45%). To eliminate any contamination of **3a** by **2a**, the product was recrystallized by dissolving the solid in ca. 100 mL of hot acetone, filtering, slowly reducing the filtrate volume, and finally

chilling the filtrate to 0 °C overnight. The green microcrystalline solid was collected by filtration and vacuum dried. Anal. Calcd for $\text{C}_{56}\text{H}_{56}\text{Cl}_4\text{O}_3\text{P}_4\text{Re}_2$ (i.e. $\text{Re}_2\text{O}_3\text{Cl}_4(\text{dppm})_2 \cdot 2(\text{CH}_3)_2\text{CO}$): C, 46.47; H, 3.91. Found: C, 46.23; H, 3.50.

The bis(acetone) solvate was also obtained when the oxygenation reaction was carried out in wet acetone. A total of 400 μL of H_2O was added to a 50-mL Schlenk tube that contained a quantity of **1a** (0.100 g, 0.078 mmol) in acetone (20 mL). A stream of O_2 gas was bubbled through the solution for 2 h. The reaction mixture was allowed to stand for 5 days during which time a crop of bright green crystals formed. These were collected by filtration, rinsed with chilled acetone (3 × 5 mL), and vacuum dried; yield 0.074 g (72%). The product was recrystallized from hot acetone (100 mL) to eliminate trace quantities of **2a**.

(b) From $\text{Re}_2(\mu\text{-O})(\mu\text{-Cl})(\text{O})\text{Cl}_3(\mu\text{-dppm})_2$. A quantity of the brown complex **2a** (0.050 g; 0.038 mmol) was dissolved in 7 mL of CH_2Cl_2 and the mixture stirred in the air at room temperature for 36 h to allow the solvent to slowly evaporate to ca. 2 mL. Diethyl ether (40 mL) was added to induce precipitation of the green complex $\text{Re}_2\text{O}_3\text{Cl}_4(\text{dppm})_2$ (**3a**). After a period of 1 h, the green solid was filtered off, washed with diethyl ether (2 × 3 mL), and vacuum dried; yield 0.028 g (55%).

(ii) X = Br (**3b**). This complex was prepared from $\text{Re}_2(\mu\text{-O})(\mu\text{-Br})(\text{O})\text{Br}_3(\mu\text{-dppm})_2$ (0.050 g, 0.033 mmol) with use of a procedure similar to the one described in section B(i)(b); yield 0.023 g (46%). The identity of this product was established through a comparison of its spectroscopic and electrochemical properties with those of the chloride derivative **3a**.

C. Synthesis of $\text{Re}_2(\mu\text{-O})(\text{O})\text{Cl}_4(\mu\text{-dppm})_2(\text{CNR})$. (i) R = C_6H_5 -2,6-Me₂ (**4a**). A solution of $\text{Re}_2(\mu\text{-O})(\mu\text{-Cl})(\text{O})\text{Cl}_3(\mu\text{-dppm})_2$ (**2a**) (0.10 g, 0.076 mmol) and xylNC (0.015 g, 0.114 mmol) in deoxygenated CH_2Cl_2 (6 mL) was stirred at room temperature for 3 h, and the blue-green solution was treated with 60 mL of *n*-pentane to induce precipitation of the title complex. The dark green solid was filtered off, washed with pentane (3 × 5 mL), and vacuum dried; yield 0.108 g (98%). Anal. Calcd for $\text{C}_{59}\text{H}_{53}\text{Cl}_4\text{NO}_3\text{P}_4\text{Re}_2$ (i.e. $\text{Re}_2(\mu\text{-O})(\text{O})\text{Cl}_4(\mu\text{-dppm})_2 \cdot (\text{CNxyl}) \cdot \text{H}_2\text{O}$): C, 48.39; H, 3.79. Found: C, 48.18; H, 3.56. The presence of lattice H_2O was confirmed by IR and ¹H NMR spectroscopy.

A different product (denoted **4a'**) was obtained as a brown microcrystalline solid upon reacting **2a** with a little less than 1 equiv of xylNC. A mixture of $\text{Re}_2(\mu\text{-O})(\mu\text{-Cl})(\text{O})\text{Cl}_3(\mu\text{-dppm})_2$ (**2a**) (0.080 g, 0.061 mmol), xylNC (0.0076 g; 0.058 mmol), and deoxygenated CH_2Cl_2 (5 mL) was stirred at room temperature for 6 h. The color changed from black-brown to green and finally to brown. This resulting brown solution was treated with 40 mL of *n*-pentane to induce the precipitation of the brown product **4a'**, which was filtered off and washed with *n*-pentane (5 mL); yield 0.072 g (82%).

This same product **4a'** can be prepared by the following alternative route. A mixture of **2a** (0.010 g, 0.0076 mmol) and **4a** (0.025 g, 0.0173 mmol) in 5 mL of deoxygenated CH_2Cl_2 was stirred at room temperature for 15 h. After this time the dark brown solution was reduced in volume to ca. 2 mL and 20 mL of *n*-pentane added to induce precipitation of brown **4a'** which was worked-up as described before; yield 0.021 g (84% based on **4a**). Anal. Calcd for $\text{C}_{59}\text{H}_{53}\text{Cl}_4\text{NO}_3\text{P}_4\text{Re}_2$ (i.e. $\text{Re}_2(\mu\text{-O})(\text{O})\text{Cl}_4(\mu\text{-dppm})_2 \cdot (\text{CNxyl})$): C, 49.00; H, 3.70; Cl, 9.81. Found: C, 47.60; H, 3.50; Cl, 9.64.

(ii) R = CHMe₂ (**4b**). This complex was obtained by the reaction of **2a** (0.10 g, 0.076 mmol) with *i*-PrNC (0.006 mL) through use of a procedure similar to that described in section C(i); yield 0.089 g (85%). Anal. Calcd for $\text{C}_{54}\text{H}_{53}\text{Cl}_4\text{NO}_3\text{P}_4\text{Re}_2$ (i.e. $\text{Re}_2(\mu\text{-O})(\text{O})\text{Cl}_4(\mu\text{-dppm})_2 \cdot (\text{CN-}i\text{-Pr})(\mu\text{-dppm})_2 \cdot \text{H}_2\text{O}$): C, 46.25; H, 3.82. Found: C, 46.08; H, 3.64. The presence of lattice H_2O was confirmed by IR and ¹H NMR spectroscopy.

(iii) R = CMe₃ (**4c**). With the same quantities of reagents as in section C(ii), the reaction of **2a** with *t*-BuNC gave the title complex; yield 0.099 g (93%). The identity of this product was based upon its cyclic voltammetric and spectroscopic properties.

(iv) R = C₆H₁₁ (**4d**). With the use of a procedure similar to that described in section C(i), **2a** (0.10 g, 0.076 mmol) and CyNC (0.007 mL) were reacted in 6 mL of CH_2Cl_2 ; yield 0.092 g (85%). Anal. Calcd for $\text{C}_{57}\text{H}_{57}\text{Cl}_4\text{NO}_3\text{P}_4\text{Re}_2$ (i.e. $\text{Re}_2(\mu\text{-O})(\text{O})\text{Cl}_4(\mu\text{-dppm})_2 \cdot (\text{CNCy}) \cdot \text{H}_2\text{O}$): C, 47.47; H, 3.99. Found: C, 46.75; H, 3.91. The presence of lattice H_2O was confirmed by IR and ¹H NMR spectroscopy.

D. Synthesis of $\text{Re}_2(\mu\text{-O})(\text{O})\text{Cl}_4(\mu\text{-dppm})_2(\text{NCMe})$ (5**).** A solution of **2a** (0.05 g, 0.038 mmol) in 3 mL of deoxygenated CHCl_3 was treated with 2 mL of acetonitrile and the mixture stirred at room temperature for 10 h. The brown precipitate was filtered off, washed with diethyl

Table I. Crystallographic Data for $\text{Re}_2(\mu\text{-O})(\mu\text{-Cl})(\text{O})\text{Cl}_3(\mu\text{-dppm})_2(\text{CH}_3)_2\text{CO}$ (**2a**· $(\text{CH}_3)_2\text{CO}$), $\text{Re}_2(\mu\text{-O})(\text{O})_2\text{Cl}_4(\mu\text{-dppm})_2\cdot 2(\text{CH}_3)_2\text{CO}$ (**3a**· $(\text{CH}_3)_2\text{CO}$), $\text{Re}_2(\mu\text{-O})(\text{O})_2\text{Cl}_4(\mu\text{-dppm})_2\cdot 2\text{CH}_2\text{Cl}_2$ (**3a**· CH_2Cl_2), and $\text{Re}_2(\mu\text{-O})(\text{O})\text{Cl}_4(\mu\text{-dppm})_2(\text{CNxyl})\cdot\text{CH}_2\text{Cl}_2\cdot\text{H}_2\text{O}$ (**4a**)

	2a · $(\text{CH}_3)_2\text{CO}$	3a · $(\text{CH}_3)_2\text{CO}$	3a · CH_2Cl_2	4a
chem formula	$\text{Re}_2\text{Cl}_4\text{P}_4\text{O}_3\text{C}_5\text{H}_{50}$	$\text{Re}_2\text{Cl}_4\text{P}_4\text{O}_5\text{C}_{56}\text{H}_{50}$	$\text{Re}_2\text{Cl}_8\text{P}_4\text{O}_3\text{C}_{52}\text{H}_{48}$	$\text{Re}_2\text{Cl}_6\text{P}_4\text{O}_3\text{NC}_{60}\text{H}_{57}$
fw	1373.1	1441.0	1500.88	1549.14
space group	$P\bar{1}$	$P\bar{1}$	$P\bar{1}$	$P\bar{1}$
a, Å	16.069(6)	11.193(2)	11.264(4)	14.316(3)
b, Å	16.540(5)	12.882(2)	11.317(4)	14.818(2)
c, Å	12.214(2)	10.892(2)	12.966(7)	16.840(2)
α , deg	109.18(2)	101.95(1)	103.86(4)	99.60(1)
β , deg	99.09(3)	113.30(1)	104.24(4)	106.38(1)
γ , deg	101.01(3)	75.52(1)	113.54(3)	97.26(1)
V, Å ³	2923(2)	1386.3(4)	1358(3)	3322(2)
Z	2	1	1	2
T, °C	23	23	20	20
λ , Å (Mo K α)	0.71069	0.71069	0.71073	0.71073
ρ_{calcd} , g cm ⁻³	1.560	1.726	1.834	1.548
μ (Mo K α), cm ⁻¹	45.23	47.75	50.67	40.68
transm coeff	1.00–0.73	1.00–0.64	1.00–0.64	1.00–0.74
R^a	0.068	0.029	0.052	0.056
R_w^b	0.082	0.058	0.072	0.082

$$^a R = \sum ||F_o| - |F_c|| / \sum |F_o|, \quad ^b R_w = \{ \sum w(|F_o| - |F_c|)^2 / \sum w|F_o|^2 \}^{1/2}; \quad w = 1/\sigma^2(|F_o|).$$

ether, and vacuum dried; yield 0.041 g (79%). The identity of this product was based upon its spectroscopic and electrochemical properties.

E. Oxidation of $\text{Re}_2(\mu\text{-O})(\text{O})\text{Cl}_4(\mu\text{-dppm})_2(\text{CNR})$ to $[\text{Re}_2(\mu\text{-O})(\text{O})\text{Cl}_4(\mu\text{-dppm})_2(\text{CNR})]\text{PF}_6$. All oxidations were carried out by use of exactly the same procedure, so details of a representative example only are given.

(i) **R = $\text{C}_6\text{H}_3\text{-2,6-Me}_2$ (**6a**).** A mixture of **4a** (0.050 g, 0.035 mmol) and $(\eta^5\text{-C}_5\text{H}_5)_2\text{Fe}[\text{PF}_6]$ (0.012 g, 0.037 mmol) in 4 mL of CH_2Cl_2 was stirred at room temperature for 30 min. The red-brown solution was treated with diethyl ether (50 mL) and a stream of N_2 passed through the solution for 10 min to induce precipitation of the oxidized product. The red-brown crystalline solid was filtered off, washed with diethyl ether (3 × 3 mL), and vacuum dried; yield 0.043 g (78%). Anal. Calcd for $\text{C}_{59}\text{H}_{53}\text{Cl}_4\text{F}_6\text{NO}_2\text{P}_3\text{Re}_2$: C, 44.53; H, 3.36. Found: C, 43.44; H, 3.27.

(ii) **R = CHMe_2 (**6b**).** Yield: 71%.

(iii) **R = CMe_3 (**6c**).** Yield: 70%.

Preparation of Single Crystals for X-ray Structure Analysis. Crystals of $\text{Re}_2(\mu\text{-O})(\mu\text{-Cl})(\text{O})\text{Cl}_3(\mu\text{-dppm})_2(\text{CH}_3)_2\text{CO}$ (**2a**· $(\text{CH}_3)_2\text{CO}$) were obtained by exposing an acetone solution of $\text{Re}_2\text{Cl}_4(\mu\text{-dppm})_2$ to the atmosphere for several days. Large brown crystals of **2a**· $(\text{CH}_3)_2\text{CO}$ were harvested by filtration. The yellow-green filtrate was then allowed to evaporate slowly in air to give a batch of good quality green single crystals of $\text{Re}_2(\mu\text{-O})(\text{O})_2\text{Cl}_4(\mu\text{-dppm})_2\cdot 2(\text{CH}_3)_2\text{CO}$ (**3a**· $(\text{CH}_3)_2\text{CO}$). The same complex was obtained with two molecules of lattice CH_2Cl_2 in place of acetone (**3a**· CH_2Cl_2) by diffusion of heptane into a dichloromethane solution of **3a**. Single crystals of composition $\text{Re}_2(\mu\text{-O})(\text{O})\text{Cl}_4(\mu\text{-dppm})_2(\text{CNxyl})\cdot\text{CH}_2\text{Cl}_2\cdot\text{H}_2\text{O}$ (**4a**) were grown from a solution of **4a** in CH_2Cl_2 /isopropyl ether.

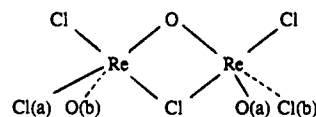
X-ray Structure Analyses. The structures of **2a**· $(\text{CH}_3)_2\text{CO}$, **3a**· $(\text{CH}_3)_2\text{CO}$, **3a**· CH_2Cl_2 , and **4a** were determined by the application of standard procedures.¹⁵ The structure determinations on **2a**· $(\text{CH}_3)_2\text{CO}$ and **3a**· $(\text{CH}_3)_2\text{CO}$ were carried out at MSU those of **3a**· CH_2Cl_2 and **4a** at PU. The basic crystallographic parameters for all four crystals are listed in Table I. The cell constants are based on 25 reflections with $20^\circ < 2\theta < 30^\circ$, $20^\circ < 2\theta < 28^\circ$, $30^\circ < 2\theta < 38^\circ$, and $32^\circ < 2\theta < 38^\circ$, respectively. Crystallographic data were collected on Rigaku AFC6S or Enraf-Nonius CAD4 diffractometers. Three standard reflections were measured after every 5000 s of beam exposure during data collection, but we observed no systematic variations in decay in these standards. Lorentz and polarization corrections were applied to all four sets of data. An empirical absorption correction¹⁶ was applied in all cases. The linear absorption coefficient used was 45.19 cm⁻¹ for **2a**· $(\text{CH}_3)_2\text{CO}$, 47.75 cm⁻¹ for **3a**· $(\text{CH}_3)_2\text{CO}$, 50.67 cm⁻¹ for **3a**· CH_2Cl_2 , and 40.68 cm⁻¹ for **4a**. No corrections for extinction were applied. Calculations were performed on a VAXSTATION 2000 computer by using the Texsan crystallographic software package of Molecular Structure Corp.¹⁷ or on a microVAX II computer using the Enraf-Nonius structure determination package.

(15) See, for example: (a) Bino, A.; Cotton, F. A.; Fanwick, P. E. *Inorg. Chem.* **1979**, *18*, 3558. (b) Cotton, F. A.; Frenz, B. A.; Deganello, G.; Shaver, A. J. *Organomet. Chem.* **1973**, *50*, 227.

(16) Walker, N.; Stuart, D. *Acta Crystallogr., Sect. A: Found Crystallogr.* **1983**, *A39*, 158.

(17) TEXSAN-TEXRAY Structure Analysis Package.

The structure of **2a**· $(\text{CH}_3)_2\text{CO}$ was solved by SHELXS-86¹⁸ and DIRDIF¹⁹ structure solution programs within the Texsan software package and was refined by full-matrix least-squares refinement. Hydrogen atoms were not included in the refinement. All non-hydrogen atoms were refined with anisotropic thermal parameters with the exception of O(2b) and the atoms of the interstitial acetone molecule; corrections for anomalous scattering were applied to anisotropically refined atoms.²⁰ Early in the refinement procedure, it became apparent that a disorder exists between the terminal O atom and a Cl atom. This is not surprising in view of the pseudo-symmetry of the molecule. In light of this symmetry, we were curious as to whether the crystal belonged to a monoclinic system rather than a triclinic system, but data collected on two independent crystals (one at Michigan State U. and one at Purdue U.) gave no indication of a higher symmetry cell. Furthermore, we employed several cell reduction programs including the Delaunay reduction TRACER²¹ and the program MISSYM,²² neither of which transformed the cell to monoclinic. The Re–O and Re–Cl distances are quite different; therefore, the two peaks appearing in the map in the same approximate vicinity near each Re center were easily assigned. In the case of O(2b), since it tended to be “absorbed” by the Cl atom after several cycles of refinement, we chose to fix its position as determined in the original difference map after the other atoms had been located. Refinement of the occupancy of the disordered positions of the Cl atom led to an exact 0.5/0.5 population between the two sites. After establishment of this ratio for the Cl atom, the occupancies for the disordered O atom were then fixed to 0.5. The following scheme depicts the arrangement of atoms in the equatorial plane containing the metal atoms:



One phenyl ring showed some high thermal parameters for certain carbon atoms which may be a manifestation of the disorder in the equatorial plane being transferred to the dppm ligands. After this modeling of the Cl/O disorder and location of the other non-hydrogen atoms in the Re_2 unit, a region of electron density appeared in the lattice which was readily assigned as an acetone molecule and fixed after several cycles because

(18) Sheldrick, G. M. In *Crystallographic Computing 3*, Sheldrick, G. M., Kruger, C., Goddard, R., Eds.; Oxford University Press: Oxford, U.K., 1985; pp 175–189.

(19) DIRDIF: Direct Methods for Difference Structure, An Automatic Procedure for Phase Extension; Refinement of Difference Structure Factors. Beurskens, R. T., Technical Report, 1984.

(20) (a) Cromer, D. T. *International Tables for X-ray Crystallography*; Kynoch: Birmingham, England, 1974; Vol. IV, Table 2.3.1. (b) For the scattering factors used in the structure solution, see: Cromer, D. T.; Waber, J. T. *Ibid.*, Table 2.2B.

(21) Lawton, S. L.; Jacobson, R. A. The Reduced Cell and Its Crystallographic Applications, United States Atomic Energy Commission, Research and Development Report, TID-4500, 1965.

(22) Page, Y. L. *J. Appl. Crystallogr.* **1988**, *21*, 983.

Table II. Positional Parameters and Equivalent Isotropic Displacement Parameters (\AA^2) for the Non-Phenyl Group Atoms of $2\mathbf{a}\cdot(\text{CH}_3)_2\text{CO}^a$

atom	x	y	z	B
Re(1)	0.84709(6)	0.74656(6)	0.21833(8)	3.02(4)
Re(2)	0.68700(6)	0.75291(6)	0.36542(8)	2.89(4)
Cl(1)	0.6852(4)	0.6985(4)	0.1432(4)	3.4(2)
Cl(2)	0.9934(4)	0.8033(4)	0.3233(6)	4.8(2)
Cl(3)	0.7002(4)	0.8052(4)	0.5696(5)	4.2(2)
Cl(4a)	0.8808(7)	0.7035(7)	0.0324(8)	2.8(4)
Cl(4b)	0.537(1)	0.714(2)	0.324(3)	5.6(7)
P(1)	0.8416(4)	0.8932(4)	0.2191(5)	3.1(2)
P(2)	0.7002(4)	0.9053(4)	0.3710(5)	3.1(2)
P(3)	0.7010(4)	0.6075(4)	0.3712(5)	3.2(2)
P(4)	0.8466(4)	0.5996(4)	0.2255(5)	3.5(2)
O(1)	0.809(1)	0.776(1)	0.363(1)	3.7(6)
O(2a)	0.580(2)	0.720(4)	0.314(5)	4(2)
O(2b)	0.8431	0.7211	0.0762	4.0*
C(49)	0.808(1)	0.954(1)	0.353(2)	3.3(8)
C(50)	0.811(1)	0.589(1)	0.358(2)	3.5(8)
O(3) ^b	0.6824	0.2634	0.3987	4.0*
C(51) ^b	0.6180	0.2569	0.4453	4.0*
C(52) ^b	0.5973	0.3360	0.5512	4.0*
C(53) ^b	0.5917	0.1792	0.4632	4.0*

^a Anisotropically refined atoms are given in the form of the isotropic equivalent thermal parameter defined as $(4/3)[a^2\beta(1,1) + b^2\beta(2,2) + c^2\beta(3,3) + ab(\cos\gamma)\beta(1,2) + ac(\cos\beta)\beta(1,3) + bc(\cos\alpha)\beta(2,3)]$. Starred values are for isotropically refined atoms. Data for the phenyl group atoms are available in the supplementary material. ^b Atom of a lattice solvent molecule.

Table III. Positional Parameters and Equivalent Isotropic Displacement Parameters (\AA^2) for the Non-Phenyl Group Atoms of $3\mathbf{a}\cdot(\text{CH}_3)_2\text{CO}^a$

atom	x	y	z	B
Re(1)	-0.16982(3)	0.04364(3)	0.01642(4)	1.82(2)
Cl(1)	-0.2719(2)	0.0212(2)	-0.2248(2)	2.8(1)
Cl(2)	-0.0456(2)	0.0611(2)	0.2567(2)	2.9(1)
P(1)	-0.1332(2)	-0.1504(2)	0.0427(2)	2.04(9)
P(2)	-0.1557(2)	0.2236(2)	-0.0212(2)	1.92(8)
O(1)	0	0	0	2.0(3)
O(2)	-0.3190(6)	0.0833(5)	0.0367(7)	3.3(3)
C(25)	-0.0463(8)	0.2044(7)	-0.116(1)	2.2(3)
O(3) ^b	0.775(1)	0.2822(9)	0.492(1)	7.0(2)*
C(26) ^b	0.714(1)	0.212(1)	0.426(1)	5.4(3)*
C(27) ^b	0.763(2)	0.096(1)	0.474(2)	6.8(4)*
C(28) ^b	0.594(2)	0.249(2)	0.294(2)	9.4(5)*

^a Anisotropically refined atoms are given in the form of the isotropic equivalent thermal parameter defined as $(4/3)[a^2\beta(1,1) + b^2\beta(2,2) + c^2\beta(3,3) + ab(\cos\gamma)\beta(1,2) + ac(\cos\beta)\beta(1,3) + bc(\cos\alpha)\beta(2,3)]$. Starred values are for isotropically refined atoms. Data for the phenyl group atoms are available in the supplementary material. ^b Atom of a lattice solvent molecule.

of large shifts in positions; presumably, this is due to the usual lack of precise packing that often occurs for lattice solvent molecules. We did not, however, observe any alternative orientations of the acetone unit that could be modeled. Several peaks above $1\text{ e}/\text{\AA}^3$ were left unassigned, as there were no chemically sensible relationships among them and the peaks were very low (the highest of them was $1.3\text{ e}/\text{\AA}^3$).

The Re(1)–O(2b) and Re(2)–O(2a) distances of 1.63 and 1.65 Å, respectively, are reasonable for terminal rhenium–oxo bond distances; likewise, the Re(1)–Cl(4a) and Re(2)–Cl(4b) separations of 2.33 and 2.30 Å are within the expected range. The presence of the Re=O terminal moiety is further supported by the observation of a $\nu(\text{Re}=\text{O})$ stretch at 907 ($\text{m}\cdot\text{s}^{-1}$) in the IR spectrum of $2\mathbf{a}$.

The structure solutions of $3\mathbf{a}\cdot(\text{CH}_3)_2\text{CO}$ and $3\mathbf{a}\cdot\text{CH}_2\text{Cl}_2$ presented no problems. The former utilized the MITHRIL²³ and DIRDIF¹⁹ structure solution programs, while for the latter the Enraf-Nonius structure solution procedure MolEN was used. Hydrogen atoms of the dppm ligands of $3\mathbf{a}\cdot(\text{CH}_3)_2\text{CO}$, and $3\mathbf{a}\cdot\text{CH}_2\text{Cl}_2$ were introduced at calculated positions (C–H = 0.95 Å, B = 1.3 B_u), not refined but constrained to ride on their C atoms. With the exception of the atoms of the lattice acetone molecules,

Table IV. Positional Parameters and Equivalent Isotropic Displacement Parameters (\AA^2) for the Non-Phenyl Group Atoms of $3\mathbf{a}\cdot\text{CH}_2\text{Cl}_2^a$

atom	x	y	z	B
Re	-0.18155(6)	-0.01478(6)	-0.04746(5)	2.10(1)
Cl(1)	-0.0771(4)	0.2331(3)	0.0331(3)	3.09(9)
Cl(2)	-0.2705(4)	-0.2655(3)	-0.1248(3)	3.1(1)
P(1)	-0.1283(4)	0.0337(4)	-0.2128(3)	2.20(9)
P(2)	0.1736(4)	0.0462(4)	-0.1345(3)	2.53(9)
O(B)	0	0	0	2.1(3)
O(T)	-0.3471(9)	-0.042(1)	-0.0929(9)	3.4(3)
C(B)	0.061(1)	0.126(1)	-0.171(1)	2.6(4)
Cl(9001) ^b	0.2343(8)	0.5244(7)	0.7825(6)	8.8(2)
Cl(9002) ^b	0.3496(7)	0.6861(8)	0.6582(7)	10.2(3)
C(9000) ^b	0.344(3)	0.685(3)	0.790(2)	9(1)

^a Anisotropically refined atoms are given in the form of the isotropic equivalent thermal parameter defined as $(4/3)[a^2\beta(1,1) + b^2\beta(2,2) + c^2\beta(3,3) + ab(\cos\gamma)\beta(1,2) + ac(\cos\beta)\beta(1,3) + bc(\cos\alpha)\beta(2,3)]$. Data for the phenyl group atoms are available in the supplementary material.

^b Atom of a lattice solvent molecule.

Table V. Positional Parameters and Equivalent Isotropic Displacement Parameters (\AA^2) for the Non-Phenyl Group Atoms of $4\mathbf{a}^a$

atom	x	y	z	B
Re(1)	0.19043(5)	0.25776(5)	0.24342(4)	2.73(2)
Re(2)	0.06951(5)	0.15986(5)	0.38758(4)	2.61(2)
Cl(11)	0.2512(3)	0.4040(3)	0.3416(3)	3.6(1)
Cl(12)	0.1264(3)	0.1060(3)	0.1527(3)	3.8(1)
Cl(13)	0.2612(3)	0.3068(4)	0.1445(3)	4.6(1)
Cl(21)	0.1431(3)	0.2990(3)	0.4978(3)	3.8(1)
P(11)	0.0396(3)	0.3240(3)	0.1994(3)	2.8(1)
P(12)	0.3406(3)	0.2137(3)	0.3270(3)	3.1(1)
P(21)	-0.0598(3)	0.2506(3)	0.3325(3)	2.8(1)
P(22)	0.2329(3)	0.1126(3)	0.4411(3)	3.0(1)
O(B)	0.1286(7)	0.2108(8)	0.3211(7)	3.1(3)
O(22)	0.0076(8)	0.1067(8)	0.4493(7)	3.6(3)
N(20)	-0.0230(9)	-0.0321(9)	0.2541(8)	3.0(3)
C(20)	0.011(1)	0.038(1)	0.2963(9)	2.5(4)
C(B1)	-0.009(1)	0.345(1)	0.2902(9)	2.9(4)
C(B2)	0.331(1)	0.199(1)	0.431(1)	3.1(4)
C(221)	-0.097(2)	-0.078(2)	0.073(1)	7.2(7)
C(261)	-0.010(2)	-0.165(1)	0.356(1)	6.4(6)
O(W) ^b	0.210(1)	0.4794(9)	0.7278(9)	6.7(4)
Cl(801) ^b	0.4254(8)	0.6265(8)	0.3310(6)	5.4(2)*
Cl(802) ^b	0.401(1)	0.580(1)	0.160(1)	10.7(5)*
Cl(901) ^b	0.399(1)	0.156(1)	0.986(1)	10.4(5)*
Cl(902) ^b	0.476(2)	0.308(2)	0.962(2)	21(1)*
C(800) ^b	0.373(2)	0.546(2)	0.241(2)	2.4(6)*
C(900) ^b	0.411(4)	0.274(4)	1.020(3)	8(1)*

^a Anisotropically refined atoms are given in the form of the isotropic equivalent thermal parameter defined as $(4/3)[a^2\beta(1,1) + b^2\beta(2,2) + c^2\beta(3,3) + ab(\cos\gamma)\beta(1,2) + ac(\cos\beta)\beta(1,3) + bc(\cos\alpha)\beta(2,3)]$. Starred values are for isotropically refined atoms. Data for the phenyl group atoms are available in the supplementary material. ^b Atom of a lattice solvent molecule.

all non-hydrogen atoms of both forms of $3\mathbf{a}$ were refined with anisotropic thermal parameters. Corrections for anomalous scattering were applied to these atoms.²⁰

The structure of $4\mathbf{a}$ was solved as described for $3\mathbf{a}\cdot\text{CH}_2\text{Cl}_2$, with the inclusion of the hydrogen atoms of the dppm and xylNC ligands at fixed positions. A lattice water molecule was refined with full occupancy about a general position, while two crystallographically independent lattice CH_2Cl_2 molecules were each refined with half occupancy. All non-hydrogen atoms except the atoms of the lattice CH_2Cl_2 molecules were refined with anisotropic thermal parameters, corrections for anomalous scattering being applied to these atoms.²⁰

Positional parameters and their errors for the important atoms of the dirhenium compounds $2\mathbf{a}\cdot(\text{CH}_3)_2\text{CO}$, $3\mathbf{a}\cdot(\text{CH}_3)_2\text{CO}$, $3\mathbf{a}\cdot\text{CH}_2\text{Cl}_2$, and $4\mathbf{a}$ are listed in Tables II–V. The most important intramolecular bond distances and angles for these four structures are given in Tables VI–VIII. Tables giving full details of the crystal data and data collection parameters, the positional parameters for all non-hydrogen and hydrogen atoms, the anisotropic thermal parameters, and complete listings of bond distances and bond angles are available as supplementary material.

(23) MITHRIL: Integrated Direct Methods Computer Program. Gilmore, C. J. *J. Appl. Crystallogr.* 1984, 17, 42.

Table VI. Important Bond Distances (Å) and Bond Angles (deg) for $2\mathbf{a}\cdot(\text{CH}_3)_2\text{CO}^a$

Distances			
Re(1)–Cl(1)	2.493(6)	Re(2)–Cl(1)	2.557(5)
Re(1)–Cl(2)	2.337(6)	Re(2)–Cl(3)	2.314(5)
Re(1)–Cl(4a)	2.331(9)	Re(2)–Cl(4b)	2.30(2)
Re(1)–P(1)	2.441(6)	Re(2)–P(2)	2.466(6)
Re(1)–P(4)	2.460(7)	Re(2)–P(3)	2.481(6)
Re(1)–O(1)	1.91(1)	Re(2)–O(1)	1.93(1)
Re(1)–O(2b)	1.634(1) ^b	Re(2)–O(2a)	1.65(4)
Re(1)–Re(2)	3.361(2)		
Angles			
Cl(1)–Re(1)–Cl(2)	169.4(2)	Cl(1)–Re(2)–Cl(3)	175.6(2)
Cl(1)–Re(1)–Cl(4a)	96.8(3)	Cl(1)–Re(2)–Cl(4b)	91.4(7)
Cl(1)–Re(1)–P(1)	88.0(2)	Cl(1)–Re(2)–P(2)	90.4(2)
Cl(1)–Re(1)–P(4)	90.1(2)	Cl(1)–Re(2)–P(3)	90.3(2)
Cl(1)–Re(1)–O(1)	78.0(4)	Cl(1)–Re(2)–O(1)	76.2(4)
Cl(1)–Re(1)–O(2b)	81.9(1)	Cl(1)–Re(2)–O(2a)	83(2)
Cl(2)–Re(1)–Cl(4a)	93.7(3)	Cl(3)–Re(2)–Cl(4b)	93.0(7)
Cl(2)–Re(1)–P(1)	90.0(2)	Cl(3)–Re(2)–P(2)	89.1(2)
Cl(2)–Re(1)–P(4)	91.3(2)	Cl(3)–Re(2)–P(3)	89.4(2)
Cl(2)–Re(1)–O(1)	91.5(4)	Cl(3)–Re(2)–O(1)	99.4(4)
Cl(2)–Re(1)–O(2b)	108.3(2)	Cl(3)–Re(2)–O(2a)	102(2)
Cl(4a)–Re(1)–P(1)	92.8(3)	Cl(4b)–Re(2)–P(2)	95.0(8)
Cl(4a)–Re(1)–P(4)	90.3(3)	Cl(4b)–Re(2)–P(3)	94.6(8)
Cl(4a)–Re(1)–O(1)	174.7(5)	Cl(4b)–Re(2)–O(1)	167.6(8)
P(1)–Re(1)–P(4)	176.6(2)	P(2)–Re(2)–P(3)	170.3(2)
P(1)–Re(1)–O(1)	88.3(4)	P(2)–Re(2)–O(1)	85.3(4)
P(1)–Re(1)–O(2b)	85.0(1)	P(2)–Re(2)–O(2a)	95(2)
P(4)–Re(1)–O(1)	88.5(4)	P(3)–Re(2)–O(1)	85.5(4)
P(4)–Re(1)–O(2b)	97.6(1)	P(3)–Re(2)–O(2a)	95(2)
O(1)–Re(1)–O(2b)	159.0(4)	O(1)–Re(2)–O(2a)	159(2)
Re(1)–O(1)–Re(2)	122.3(7)	Re(1)–Cl(1)–Re(2)	83.4(2)

^a Numbers in parentheses are estimated standard deviations in the least significant digits. ^b The low esd for this distance is a consequence of fixing the position of the disordered oxygen atom O(2b) during the refinement (see Experimental Section).

Physical Measurements. IR spectra were recorded as mineral oil (Nujol) mulls with the use of Nicolet 740, Perkin-Elmer 599, or Perkin-Elmer 1800 FTIR spectrometers. Electronic absorption spectra were measured with Hitachi U-2000 or IBM Instruments 9420 UV–visible spectrophotometers. Electrochemical measurements were carried out on dichloromethane solutions that contained 0.1 M tetra-*n*-butylammonium hexafluorophosphate (TBAH) or tetra-*n*-butylammonium tetrafluoroborate as supporting electrolyte. $E_{1/2}$ values, determined as $(E_{p,a} + E_{p,c})/2$, were referenced to the silver/silver chloride (Ag/AgCl) electrode at room temperature and are uncorrected for junction potentials. Under our experimental conditions $E_{1/2} = +0.47$ V vs Ag/AgCl for the ferrocenium/ferrocene couple. Voltammetric experiments were performed with a BAS Inc. Model CV-27 instrument or EG&G Princeton Applied Research Model 362 scanning potentiostat in conjunction with a BAS Model RXY recorder. All NMR spectra were recorded on CD_2Cl_2 or CDCl_3 solutions of the complexes. The $^{31}\text{P}\{^1\text{H}\}$ spectra were obtained with use of a Varian XL-200A spectrometer operated at 80.98 MHz or Varian 300 or GE QE-300 (equipped with a multinuclear Quad probe) spectrometers operated at 121.5 MHz. ^1H NMR spectra were obtained with GE QE-300 and Varian 300 spectrometers operated at 300 MHz. Phosphorus resonances were referenced externally to 85% H_3PO_4 , the proton resonances to the residual protons in the incompletely deuteriated solvents (CD_2Cl_2 , $\delta +5.32$; CDCl_3 , $\delta +7.26$). Magnetic susceptibility measurements were carried out on dichloromethane solutions by the Evans method²⁴ with use of a GE QE-300 spectrometer. Variable-temperature magnetic susceptibility measurements on solid samples were carried out on a Quantum Design MPMS susceptometer housed in the Physics and Astronomy Department at Michigan State University.

Elemental microanalyses were performed by Dr. H. D. Lee of the Purdue University Microanalytical Laboratory or by Desert Analytics of Tucson, AZ.

Results

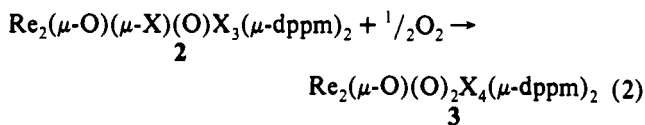
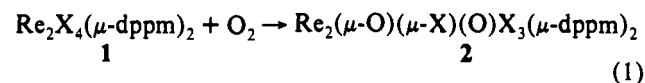
The reactions of $\text{Re}_2\text{X}_4(\mu\text{-dppm})_2$ ($1\mathbf{a}$, $\text{X} = \text{Cl}$; $1\mathbf{b}$, $\text{X} = \text{Br}$) with O_2 proceed to give dirhenium complexes of types 2 and 3

Table VII. Comparison of the More Important Bond Distances (Å) and Bond Angles (deg) for $3\mathbf{a}\cdot(\text{CH}_3)_2\text{CO}$ and $3\mathbf{a}\cdot\text{CH}_2\text{Cl}_2^a$

$3\mathbf{a}\cdot(\text{CH}_3)_2\text{CO}$		$3\mathbf{a}\cdot\text{CH}_2\text{Cl}_2$	
Distances			
Re(1)–Cl(1)	2.402(2)	Re(1)–Cl(1)	2.387(4)
Re(1)–Cl(2)	2.422(2)	Re(1)–Cl(2)	2.435(4)
Re(1)–P(2)	2.487(2)	Re(1)–P(1)	2.488(4)
Re(1)–P(1)	2.489(2)	Re(1)–P(2)	2.454(4)
Re(1)–O(1)	1.9115(5)	Re(1)–O(B)	1.9097(7)
Re(1)–O(2)	1.708(6)	Re(1)–O(T)	1.68(1)
Angles			
Cl(1)–Re(1)–Cl(2)	174.23(8)	Cl(1)–Re(1)–Cl(2)	175.7(2)
Cl(1)–Re(1)–P(2)	82.61(8)	Cl(1)–Re(1)–P(1)	81.8(1)
Cl(1)–Re(1)–P(1)	95.77(8)	Cl(1)–Re(1)–P(2)	95.5(1)
Cl(1)–Re(1)–O(1)	89.24(6)	Cl(1)–Re(1)–O(B)	90.1(1)
Cl(1)–Re(1)–O(2)	92.6(2)	Cl(1)–Re(1)–O(T)	94.6(4)
Cl(2)–Re(1)–P(2)	96.58(8)	Cl(2)–Re(1)–P(1)	97.7(1)
Cl(2)–Re(1)–P(1)	83.63(8)	Cl(2)–Re(1)–P(2)	83.9(1)
Cl(2)–Re(1)–O(1)	84.99(6)	Cl(2)–Re(1)–O(B)	85.6(1)
Cl(2)–Re(1)–O(2)	93.1(2)	Cl(2)–Re(1)–O(T)	89.7(4)
P(1)–Re(1)–P(2)	166.04(7)	P(1)–Re(1)–P(2)	166.1(1)
P(2)–Re(1)–O(1)	83.88(5)	P(1)–Re(1)–O(B)	83.92(9)
P(2)–Re(1)–O(2)	96.3(2)	P(1)–Re(1)–O(T)	97.2(4)
P(1)–Re(1)–O(1)	82.24(5)	P(2)–Re(1)–O(B)	82.4(1)
P(1)–Re(1)–O(2)	97.6(2)	P(2)–Re(1)–O(T)	96.7(4)
O(1)–Re(1)–O(2)	178.1(2)	O(B)–Re(1)–O(T)	175.3(4)
Re(1)–O(1)–Re(1)'	180.0	Re(1)–O(B)–Re(1)'	180.0

^a Numbers in parentheses are estimated standard deviations in the least significant digits. Comparisons are given between the corresponding bond distances and angles in the two structures.

as represented in eqs 1 and 2. The reaction shown in eq 1 can



be carried out in CHCl_3 , acetone, benzene, or toluene with the use of air or pure O_2 and with reaction times of a few hours. In these instances, the isolation of dark brown $2\mathbf{a}$ ($\text{X} = \text{Cl}$) and $2\mathbf{b}$ ($\text{X} = \text{Br}$) is aided by the precipitation of the complexes. Reaction of 1 with O_2 in CH_2Cl_2 gives 2 when diethyl ether is added after 2 h to precipitate 2 ; otherwise 2 reacts further with O_2 to give increasing quantities of the green complex of type 3 . Interestingly, the deliberate addition of water to an acetone solution of $1\mathbf{a}$ followed by purging with O_2 aids in the solubilization of the initial product $2\mathbf{a}$ which then goes on to form $3\mathbf{a}$ in high yield. As far as we could tell, in none of the aforementioned systems was water found to be the source of the oxygen in complexes 2 and 3 . The course of the reactions were not affected in any significant way by different degrees of drying of the solvents. In one experiment, a solution of $1\mathbf{a}$ in acetone was treated with a small quantity of water with strict exclusion of O_2 . After a period of 60 days, it was evident that no reaction had occurred as judged by the persistence of the characteristic purple color of the parent complex. When this mixture was then exposed to air, large bright green crystals of $3\mathbf{a}$ formed within several days following the formation of a wine-red coloration due to the intermediate formation of $2\mathbf{a}$. Furthermore, when a sample of $2\mathbf{a}$ was dissolved in CD_2Cl_2 and treated with a trace of H_2O , we found that H_2 was not evolved, thereby ruling out the occurrence of the redox reaction $\text{Re}_2(\mu\text{-O})(\mu\text{-Cl})(\text{O})\text{Cl}_3(\mu\text{-dppm})_2 + \text{H}_2\text{O} \rightarrow \text{Re}_2(\mu\text{-O})(\text{O})_2\text{Cl}_4(\mu\text{-dppm})_2 + \text{H}_2$ as being the origin of the conversion of 2 to 3 .

When tetrahydrofuran was used as the reaction solvent, 1 reacted with air or O_2 to give 2 , followed by 3 , but it proved more difficult to isolate 2 free from 3 so this is not the preferred solvent

Table VIII. Important Bond Distances (Å) and Bond Angles (deg) for **4a**^a

Distances			
Re(1)–Cl(11)	2.389(5)	Re(2)–P(21)	2.484(5)
Re(1)–Cl(12)	2.403(5)	Re(2)–P(22)	2.492(5)
Re(1)–Cl(13)	2.345(5)	Re(2)–O(B)	1.79(1)
Re(1)–P(11)	2.459(5)	Re(2)–O(22)	1.76(1)
Re(1)–P(12)	2.446(5)	Re(2)–C(20)	2.07(2)
Re(1)–O(B)	1.94(1)	N(20)–C(20)	1.12(2)
Re(2)–Cl(21)	2.424(5)	N(20)–C(21)	1.41(2)
Angles			
Cl(11)–Re(1)–Cl(12)	175.9(2)	Cl(21)–Re(2)–O(B)	88.8(4)
Cl(11)–Re(1)–Cl(13)	93.2(2)	Cl(21)–Re(2)–O(22)	93.4(4)
Cl(11)–Re(1)–P(11)	83.2(2)	Cl(21)–Re(2)–C(20)	177.4(5)
Cl(11)–Re(1)–P(12)	84.2(2)	P(21)–Re(2)–P(22)	162.3(2)
Cl(11)–Re(1)–O(B)	89.8(4)	P(21)–Re(2)–O(B)	83.2(4)
Cl(12)–Re(1)–Cl(13)	90.8(2)	P(21)–Re(2)–O(22)	96.1(4)
Cl(12)–Re(1)–P(11)	97.2(2)	P(21)–Re(2)–C(20)	97.8(5)
Cl(12)–Re(1)–P(12)	94.5(2)	P(22)–Re(2)–O(B)	82.7(4)
Cl(12)–Re(1)–O(B)	86.1(4)	P(22)–Re(2)–O(22)	98.5(4)
Cl(13)–Re(1)–P(11)	96.0(2)	P(22)–Re(2)–C(20)	93.3(5)
Cl(13)–Re(1)–P(12)	95.0(2)	O(B)–Re(2)–O(22)	177.6(5)
Cl(13)–Re(1)–O(B)	176.9(3)	O(B)–Re(2)–C(20)	91.9(6)
P(11)–Re(1)–P(12)	163.7(2)	O(22)–Re(2)–C(20)	85.9(6)
P(11)–Re(1)–O(B)	84.1(3)	Re(1)–O(B)–Re(2)	176.0(7)
P(12)–Re(1)–O(B)	85.5(3)	C(20)–N(20)–C(21)	170(2)
Cl(21)–Re(2)–P(21)	84.8(2)	Re(2)–C(20)–N(20)	172(2)
Cl(21)–Re(2)–P(22)	84.4(2)		

^a Numbers in parentheses are estimated standard deviations in the least significant digits.

for the preparation of the former complex in bulk quantities. While **1a** showed no reaction in THF or THF/H₂O mixtures in the complete absence of O₂, atypical behavior was observed when **1a** was reacted with O₂ in THF in a system that had been freed of traces of adventitious water.²⁵ Although reaction proceeded as normal to produce a wine-red solution of **2a** within a couple of hours, the solution color then changed through orange-brown to orange within 1 week and finally to a pale yellow color. Identical behavior was found when preformed **2a** was reacted with O₂ in THF under these exact same anhydrous conditions. While the nature of the products is at present unknown, these observations indicate that, at least in THF, trace amounts of water may be important for the clean conversion of **2** to **3**, but the mechanistic interpretation is uncertain and will be the subject of future investigations.

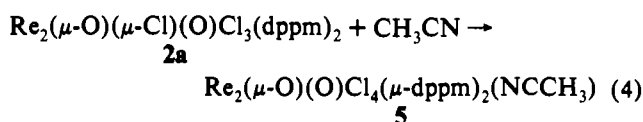
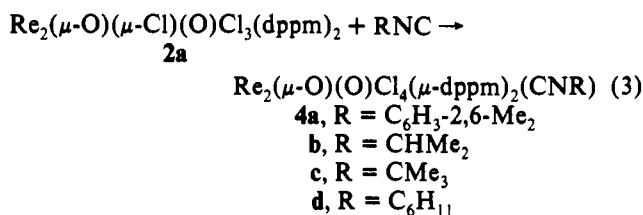
The dirhenium(IV) complexes Re₂(μ-O)(μ-X)(O)X₃(μ-dppm)₂ (**2**) display characteristic ν(Re=O) and ν(Re–O–Re) modes in their IR spectra at 907 m⁻¹ and 774 m⁻¹ for X = Cl (**2a**) and 911 m⁻¹ and 775 m⁻¹ for X = Br (**2b**). If the IR sample of **2** is prepared in air, or if the reaction to produce **2** is carried out in air, the spectra of **2** exhibit a ν(OH) mode at ca. 3630 cm⁻¹ due to lattice H₂O. Both **2a** and **2b** show very similar electrochemical properties as measured by the cyclic voltammetric (CV) technique (sweep rate *v* = 200 mV s⁻¹) on solutions in 0.1 M TBAH–CH₂Cl₂. For **2a**, the processes are E_{p,a} = +1.46, E_{1/2}(ox) = +0.47, and E_{p,c} = –0.91 V vs Ag/AgCl. In the case of the bromide analogue **2b**, the CV shows E_{p,a} = +1.35, E_{1/2}(ox) = +0.47, and E_{p,c} = –0.81 V vs Ag/AgCl, as well as coupled processes at E_{p,c} = –0.98 and E_{p,a} = –0.90 V which may be associated with a chemical product formed following the irre-

versible reduction at –0.81 V. For the oxidation at E_{1/2} +0.47 V in the CV of both **2a** and **2b**, *i*_{p,a}/*i*_{p,c} = 1.0 and ΔE_p (E_{p,a} – E_{p,c}) = 70–80 mV. Overall, these data leave little doubt that **2a** and **2b** are structurally very similar.

A magnetic moment determination on a CH₂Cl₂ solution of **2a** at room temperature by the Evans method²⁴ indicated that this complex is weakly paramagnetic (μ_{eff} = 1.0 μ_B), a conclusion that was supported by a SQUID measurement on crystalline **2a**. The μ_{eff} value is 1.13 μ_B at 280 K and at the lowest temperature measured (5 K) it is 0.42 μ_B. In accord with this behavior we were unable to locate the phosphorus resonance in the ³¹P{¹H} NMR spectrum of this complex, while the ¹H NMR spectrum (recorded in CD₂Cl₂) consisted of a series of fairly broad resonances between δ +6.2 and +12.2 (the most downfield of which were at δ +12.07, +11.48, and +9.88). These features are consistent with a Knight-shifted spectrum. Variable-temperature spectra down to –90 °C did not significantly improve the resolution of the signals.

The structural identity of **2a** as an edge-shared bioctahedral species was established by a single-crystal X-ray structure analysis of **2a**·(CH₃)₂CO. An ORTEP representation of the structure is given in Figure 1, while crystallographic data and important structural parameters are available in Tables I, II, and VI and the supplementary material. A disorder between one of the terminal chloro ligands and the terminal oxo ligand complicated the structure refinement but was modeled satisfactorily.

As a further check on the correctness of our conclusions concerning the structure **2a**, we derivatized this complex with organic isocyanides and acetonitrile. The reactions of **2a** with RNC and CH₃CN proceed as shown in eqs 3 and 4.



The crystal structure of the xylyl isocyanide derivative **4a** confirms that the Re₂(O)₂Cl₄(μ-dppm)₂ unit has been retained but shows that the coordination of the isocyanide ligand has induced a switch from the edge-shared bioctahedral structure of **2a** to a corner-shared bioctahedron in which two octahedra are joined through a single oxo bridge. The ORTEP representation of this structure is shown in Figure 2, while crystallographic data and important structural parameters are given in Tables I, V, and VIII.

The IR spectral data and the cyclic voltammetric properties of **4** and **5** are summarized in Table IX. Like **2**, these complexes show both ν(Re=O) and ν(Re–O–Re) modes. Additionally, they display ν(N≡C) or ν(C≡N) ligand modes. The redox properties of these complexes were measured by the CV technique (*v* = 200 mV s⁻¹). There are two oxidations, which have *i*_{p,a}/*i*_{p,c} ratios of 1.0 and ΔE_p values in the ranges 60–80 mV for E_{1/2}(ox)(1) and 80–130 mV for E_{1/2}(ox)(2), and a reduction at ca. –0.8 V. In some instances, the latter process approaches reversibility (*i*_{p,a} ≈ *i*_{p,c}, ΔE_p = 60–100 mV), but in the case of **4a** and **5** it is clearly irreversible with a coupled oxidation wave appearing at E_{p,a} = –0.09 and –0.15 V vs Ag/AgCl, respectively, due to a chemical product of the reduction. The potentials of the two oxidations and one reduction for **4** and **5** are very close to the values cited previously for **2a** (+1.46, +0.47, and –0.91 V, respectively).

(25) In this study, the glassware was first treated with a 1% solution of Glassclad 18, which is a hydrophobic coating for glass and limits the possibility of H₂O adhering to the surface, prior to oven drying. The O₂ gas was passed through a drying column consisting of indicating Drierite and 5-Å molecular sieves. Tetrahydrofuran was selected as the reaction solvent because distillation from sodium/potassium benzophenone ketyl radical is highly effective at eliminating H₂O. A 50-mL Schlenk tube containing 0.060 g of Re₂Cl₄(dppm)₂ and 10 mL of THF was purged with O₂ gas for 1.5 h during which time the solution color turned to a wine-red color due to the formation of **2a**. Further observations are as described in the text.

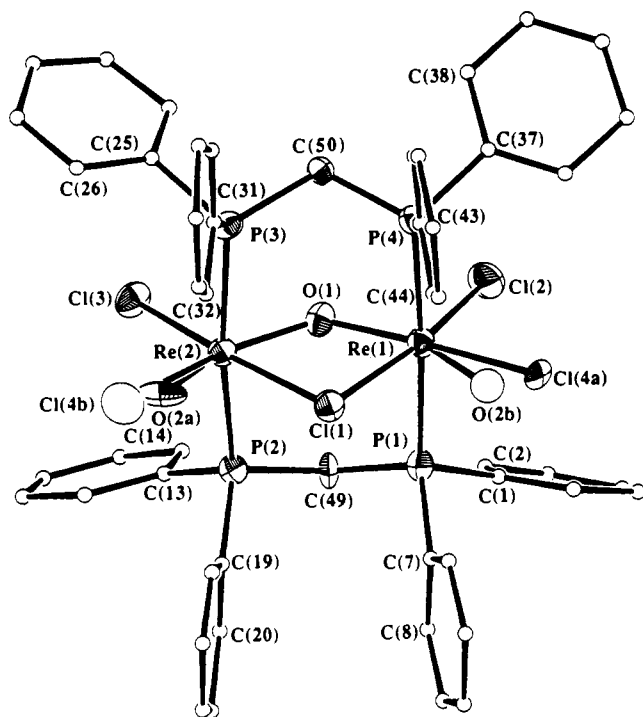


Figure 1. ORTEP representation of the structure of the molecule $\text{Re}_2(\mu\text{-O})(\mu\text{-Cl})(\text{O})\text{Cl}_3(\mu\text{-dppm})_2$ (**2a**· $(\text{CH}_3)_2\text{CO}$) showing the disorder involving the terminal chloro and oxo ligands. The thermal ellipsoids are drawn at the 35% probability level except for the phenyl group carbon atoms, which are drawn as spheres of 0.1-Å radius.

The magnetic moment of a CH_2Cl_2 solution of the xyllyl isocyanide complex **4a** was determined by the Evans method²⁴ to be $0.9 \mu_B$. For a solid sample μ_{eff} decreased from $1.09 \mu_B$ at 280 K to $0.26 \mu_B$ at 5 K, behavior which is almost the same as that for **2a**. This weak paramagnetism leads to Knight shifting in the NMR spectra. $^{31}\text{P}\{^1\text{H}\}$ NMR spectral measurements (recorded in CD_2Cl_2) on **4a-c** revealed a broad unstructured upfield resonance at δ -286, -288, and -299, respectively, which we assume is a Knight-shifted phosphorus signal for these complexes; no such resonance was observed in the spectrum of **2a**. The $^{31}\text{P}\{^1\text{H}\}$ NMR spectrum of **5** has a resonance at δ -143 which we tentatively assign in a similar way. The ^1H NMR spectra of **4a-d** (recorded in CD_2Cl_2) are very similar, each showing resonances very close to δ +12.0 and +11.7 (both doublets of relative intensity 4), a series of well-resolved multiplets between δ +9.0 and +7.0, and a broad ABX₄ type of pattern with components at δ ca +4.4 and +3.0 (intensity 4) which is typical of the methylene protons of the μ -dppm ligands. Additionally, there are resonances due to the coordinated RNC ligands. For **4a-c** these are well resolved and appear at δ +6.76 (d, C_6H_3), +6.40 (t, C_6H_3) and +1.07 (s, $-\text{CH}_3$) for **4a**, δ +5.80 (sp, CHMe_2) and +0.13 (d, CHMe_2) for **4b**, and δ +0.23 (s, $-\text{CMe}_3$) for **4c**. However, the cyclohexyl group of **4d** gives only broad poorly resolved features. The spectrum of **5** is very similar to those of its isocyanide analogues, except that the downfield doublets are much closer to one another (at δ +12.33 and +12.20) and the methyl resonance of the acetonitrile ligand is found as a sharp singlet at δ +1.97.

When the reaction shown between **2a** and xyllyl isocyanide (eq 3) is carried out with less than 1 equiv of xylNC, a product is formed (denoted **4a'**) which has properties similar but not identical to those of **4a**. It is also formed upon reacting **4a** with approximately one-half an equivalent of **2a**. Its IR spectrum (Nujol mull) exhibits a $\nu(\text{N}\equiv\text{C})$ mode at 2071 s cm^{-1} , $\nu(\text{Re}-\text{O})$ at 924 m-s cm^{-1} , and $\nu(\text{Re}-\text{O}-\text{Re})$ at 804 s cm^{-1} (shoulder at $\approx 785 \text{ cm}^{-1}$) and is therefore different from the spectrum of **4a**. Also, the CV's of **4a** and **4a'** differ, with that of **4a'** possessing the following processes: $E_{1/2}(\text{ox})(2) = +1.33$, $E_{1/2}(\text{ox})(1) =$

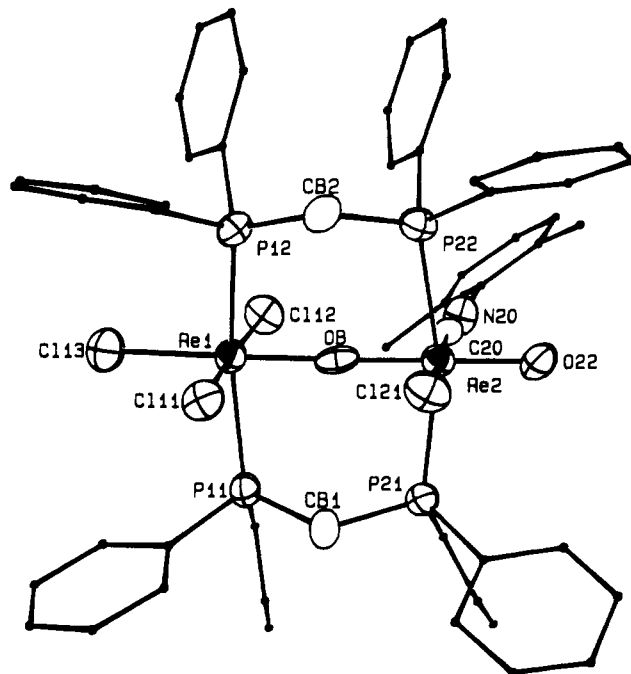


Figure 2. ORTEP representation of the structure of the molecule $\text{Re}_2(\mu\text{-O})(\text{O})\text{Cl}_4(\mu\text{-dppm})_2(\text{CNxyl})$ (**4a'**). The thermal ellipsoids are drawn at the 50% probability level except for the phenyl group carbon atoms of the dppm ligands and the carbon atoms of the xyl group, which are drawn as circles of arbitrary radius.

+0.62, $E_{1/2}(\text{red}) = -0.50 \text{ V vs Ag/AgCl}$. The ^1H NMR spectrum of **4a'** (in CD_2Cl_2 and CDCl_3) is Knight-shifted, but even more so than the corresponding spectrum of **4**. Most diagnostic of the spectrum of this complex (as recorded in CD_2Cl_2) are doublets at δ +16.47, +14.79, +13.59, +0.09, and -3.65, as well as a complex pattern between δ +9.8 and +4.6. At the present time we have made no attempt to assign this very complicated spectrum. The structural relationship between **4a'** and **4a** remains to be established.

The reversible oxidation of **4** at ca. +0.3 V (Table IX) can be accessed chemically by the use of $[(\eta^5\text{-C}_5\text{H}_5)_2\text{Fe}]\text{PF}_6$ in CH_2Cl_2 as shown by the conversion of **4a-c** to the corresponding one-electron oxidized salts $[\text{Re}_2(\mu\text{-O})(\text{O})\text{Cl}_4(\mu\text{-dppm})_2(\text{CNR})]\text{PF}_6$ (**6a-c**). These complexes display $\nu(\text{N}\equiv\text{C})$ modes only slightly higher ($<20 \text{ cm}^{-1}$) than those in the neutral parent species, while the $\nu(\text{Re}=\text{O})$ mode is tentatively assigned to the band at ca. 805 cm^{-1} although a broad weak band at ca. 935 cm^{-1} could be an alternative candidate (see Discussion). The $\nu(\text{P}-\text{F})$ mode of the $[\text{PF}_6]^-$ anion is at 845 s cm^{-1} . The oxidation of **4** to **6** is accompanied by a marked increase in the paramagnetism of the compounds as shown by magnetic susceptibility measurements on the xyllyl isocyanide complex **6a**. The magnetic moment of a CH_2Cl_2 solution of this complex as measured by the Evans method,²⁴ is ca. $2.7 \mu_B$ while for the solid complex a SQUID measurement gave $\mu_{\text{eff}} = 3.23 \mu_B$ at 280 K and $2.47 \mu_B$ at 5 K. A plot of $1/\chi_M$ against T shows close to Curie law behavior. The CV properties of these complexes are the same as those of the parent species **4** except that the process at $E_{1/2}$ ca. +0.3 V now corresponds to a reduction of the bulk complex.

The diamagnetic dirhenium(V) complexes $\text{Re}_2(\mu\text{-O})(\text{O})_2\text{X}_4(\mu\text{-dppm})_2$ (**3a**, $\text{X} = \text{Cl}$; **3b**, $\text{X} = \text{Br}$), which are formed as shown in eq 2, have IR spectra and electrochemical properties that are very similar for both complexes. Thus, the Nujol mull IR spectrum of **3a** shows $\nu(\text{Re}=\text{O})$ at 802 m and 785 m cm^{-1} and $\nu(\text{Re}-\text{O}-\text{Re})$ at 715 s cm^{-1} . The CV of a solution of **3a** in 0.1 M TBAH- CH_2Cl_2 shows an oxidation at $E_{1/2}(\text{ox}) = +1.30 \text{ V}$ and an irreversible reduction at $E_{p,c} = -0.88 \text{ V vs Ag/AgCl}$ with a coupled $E_{p,a}$ process at -0.78 V ($i_{p,a} < i_{p,c}$). There is an additional process at $E_{p,c} \approx -0.10 \text{ V}$ due to the formation of a chemical product following the irreversible reduction at -0.88 V . The

Table IX. Selected Electrochemical and IR Spectral Data for Isocyanide and Nitrile Adducts of the Type $\text{Re}_2(\mu\text{-O})(\text{O})\text{Cl}_4(\mu\text{-dppm})_2(\text{L})$ (**4** and **5**) and Their Oxidized Congeners $[\text{Re}_2(\mu\text{-O})(\text{O})\text{Cl}_4(\mu\text{-dppm})_2(\text{L})]\text{PF}_6$ (**6**)

complex	L	IR spectral data, cm^{-1} ^a			CV half-wave potentials, V ^{c,d}			
		$\nu(\text{N}\equiv\text{C})/\nu(\text{C}\equiv\text{N})$	$\nu(\text{Re}=\text{O})$	$\nu(\text{Re}-\text{O}-\text{Re})$	$E_{1/2}(\text{ox})(1)$	$E_{1/2}(\text{ox})(2)$	$E_{1/2}(\text{red})$	other processes
4a	xylnC	2148 s	863 s	774 m	+1.46(130)	+0.33(70)	-0.82 ^e	$E_{\text{p,a}} = -0.09$ ^f
4b	Me_2CHNC	2194 s	867 s	≈ 780 sh, 768 m	+1.44(100)	+0.30(70)	-0.83(80)	
4c	Me_3CNC	2185 s	869 s	≈ 780 sh, 765 m	+1.49(130)	+0.30(80)	-0.86(100)	
4d	$\text{C}_6\text{H}_5\text{NC}$	2192 s	867 s	≈ 780 sh, 768 m	+1.47(80)	+0.32(60)	-0.82(60)	
5	CH_3CN	2282 vw, 2249 w	914 s	781 s	+1.24(80)	+0.47(80)	-0.77 ^e	$E_{\text{p,a}} = -0.15$ ^f
6a	xylnC	2152 m-s	<i>b</i>	779 m	+1.46(130)	+0.33(70) ^g	-0.82 ^e	$E_{\text{p,a}} = -0.10$ ^f
6b	Me_2CHNC	2210 m-s	<i>b</i>	777 m	+1.46(140)	+0.31(70) ^g	-0.81(70)	
6c	Me_3CNC	2202 m-s	<i>b</i>	779 m	+1.46(100)	+0.28(80) ^g	-0.88(120)	

^a Recorded as Nujol mulls. For complexes that contain the $[\text{PF}_6]$ anion there is a $\nu(\text{P}-\text{F})$ mode at ca. 845 cm^{-1} . ^b See Results and Discussion sections. ^c Measured on 0.1 M TBAH- CH_2Cl_2 solutions and referenced to the Ag/AgCl electrode with a scan rate (ν) of 200 mV/s at a Pt-bead electrode. Under our experimental conditions $E_{1/2} = +0.47$ V vs Ag/AgCl for the ferrocenium/ferrocene couple. ^d Numbers in parentheses are ΔE_p (i.e. $E_{\text{p,a}} - E_{\text{p,c}}$) in mV. ^e $E_{\text{p,c}}$ value. ^f Process associated with the formation of a chemical product. ^g $E_{1/2}(\text{red})$ value.

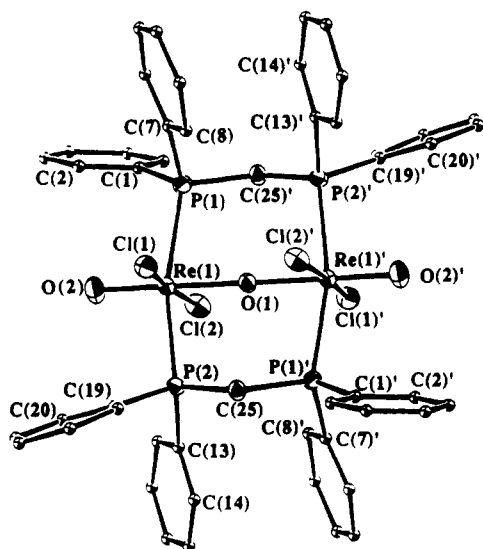


Figure 3. ORTEP representation of the structure of the molecule $\text{Re}_2(\mu\text{-O})(\text{O})_2\text{Cl}_4(\mu\text{-dppm})_2(\mathbf{3a}\cdot(\text{CH}_3)_2\text{CO})$. The thermal ellipsoids are drawn at the 40% probability level except for the phenyl group carbon atoms, which are drawn as spheres of 0.1-Å radius.

³¹P{¹H} NMR spectrum of this complex (recorded in CD_2Cl_2) consists of a singlet at $\delta -14.5$, while its ¹H NMR spectrum comprises sets of multiplets at δ ca. +7.7, ca. +7.3, and ca. +7.2 for the phenyl protons and a binomial pentet at $\delta +4.09$ for the $-\text{CH}_2-$ protons of the $\mu\text{-dppm}$ ligands.

The structure of **3a** was established from single-crystal X-ray structure analyses of two forms of this complex that contained different lattice solvent molecules ($\mathbf{3a}\cdot(\text{CH}_3)_2\text{CO}$ and $\mathbf{3a}\cdot\text{CH}_2\text{Cl}_2$). The structure of **3a** is, like that of **4a**, a corner-sharing bioctahedron, but unlike **4a** this molecule is centrosymmetric with identical environments about the two Re centers. An ORTEP representation of the $\text{Re}_2(\mu\text{-O})(\text{O})_2\text{Cl}_4(\mu\text{-dppm})_2$ molecule as present in $\mathbf{3a}\cdot(\text{CH}_3)_2\text{CO}$ is shown in Figure 3. The structure of this molecule in $\mathbf{3a}\cdot\text{CH}_2\text{Cl}_2$ is shown in Figure S1 (supplementary material). Crystallographic data and important structural parameters for $\mathbf{3a}\cdot(\text{CH}_3)_2\text{CO}$ and $\mathbf{3a}\cdot\text{CH}_2\text{Cl}_2$ are given in Tables I, III, IV, and VII.

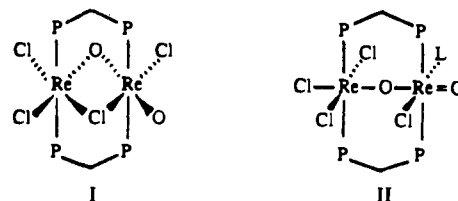
Discussion

The conversions of **1** to the dirhenium complexes **2** and **3** constitute rare instances where an authentic, structurally characterized, multiply bonded dimetal complex has reacted with molecular oxygen to give products in which the ligand integrity of the starting material is fully retained. Another example is the conversion of Ru_2R_6 compounds to $\text{Ru}_2(\mu\text{-O})_2\text{R}_6$ by molecular

O_2 .²⁶ Also, the dimolybdenum(II) compound $\text{Mo}_2(\text{S}_2\text{CNEt}_2)_4$, which was prepared many years ago^{27,28} but has not yet been fully characterized structurally, can be converted into $\text{Mo}_2\text{O}_3\text{-}(\text{S}_2\text{CNEt}_2)_4$ upon its reaction with O_2 .^{27,29}

A single-crystal X-ray structure determination of the chloro complex **2a** ($\text{CH}_3)_2\text{CO}$ shows clearly that it is an edge-sharing bioctahedron in which the $\text{Re}_2(\mu\text{-dppm})_2$ unit is still present (Figure 1). While the refinement of two terminal chlorines Cl(2) and Cl(3) and the bridging chlorine (Cl(1)) and bridging oxygen (O(1)) atoms proceeded satisfactorily, the chlorine atom Cl(4) and terminal oxygen atom O(2) were disordered. However, we were able to model this disorder satisfactorily. The terminal and bridging Re-O bonds had distances of ca. 1.63 and ca. 1.92 Å, respectively. These values are in reasonably good agreement with those found in the structures of **3a** and **4a**, in which there is no disorder, although the Re=O distance of 1.63 Å is shorter than expected, a likely consequence of some inadequacies in our modeling of the disorder. We note that disorder involving chloro and oxo ligands is a well recognized phenomenon,^{30,31} although in the case of **2a** it cannot be attributed to compositional disorder.³¹ The Re...Re distance of 3.361(2) Å in **2a**· $(\text{CH}_3)_2\text{CO}$ accords with the absence of any direct Re-to-Re interaction. This distance is in marked contrast to the short Re-Re contact of 2.522(1) Å in the symmetric dirhenium(IV) complex $\text{Re}_2(\mu\text{-O}_2\text{CC}_2\text{H}_5)(\mu\text{-O})(\mu\text{-Cl})\text{Cl}_4(\text{PPh}_3)_2$,³² a value which is consistent with the presence of a fairly strong Re-Re bond. In the di- μ -oxo bridged dirhenium(IV) complexes $\text{K}_4[\text{Re}_2(\mu\text{-O})_2(\text{C}_2\text{O}_4)_4]\cdot 3\text{H}_2\text{O}$,³³ $[\text{Re}_2(\mu\text{-O})_2\text{Cl}_2\text{L}_2]\text{I}_2\cdot 2\text{H}_2\text{O}$,³⁴ and $[\text{Re}_2(\mu\text{-O})_2\text{I}_2\text{L}_2]\text{I}_2\cdot 2\text{H}_2\text{O}$,³⁵ where L is 1,4,7-triazacyclononane, the Re-Re distances are even shorter at 2.362(1), 2.376(2), and 2.381(1) Å, respectively.

The structure of **2a** can be represented as in I. This is further supported by (1) the presence of $\nu(\text{Re}=\text{O})$ and $\nu(\text{Re}-\text{O}-\text{Re})$



modes in the IR spectra of **2a** and **2b** and (2) the derivatization of **2a** with isocyanide ligands and acetonitrile to produce the unsymmetrical compounds (II) in which the two metal centers are in quite disparate ligand environments, viz., $\text{Cl}_2\text{Re}(\mu\text{-O})(\mu\text{-dppm})_2\text{Re}(\text{O})\text{Cl}(\text{L})$. The single-crystal X-ray structure deter-

- (26) Tooze, R. P.; Wilkinson, G.; Motevalli, M.; Hursthouse, M. B. *J. Chem. Soc., Dalton Trans.* **1986**, 2711.
 (27) Steele, D. F.; Stephenson, T. A. *Inorg. Nucl. Chem. Lett.* **1973**, 9, 777.
 (28) Vella, P.; Zubietta, J. *J. Inorg. Nucl. Chem.* **1978**, 40, 477.
 (29) Baird, D. M.; Croll, S. D. *Polyhedron* **1986**, 5, 1931.
 (30) Calviou, L. J.; Arber, J. M.; Collison, D.; Garner, C. D.; Clegg, W. *J. Chem. Soc., Chem. Commun.* **1992**, 654.

mination on **4a** ($L = \text{xyINC}$) shows the presence of a linear $\text{Cl}-\text{Re}-\text{O}-\text{Re}=\text{O}$ unit (the angles range from 176.0 to 177.6°) and demonstrates the remarkable versatility of the dppm ligand in bridging both very short $\text{M}-\text{M}$ bonds (ca. 2.2 Å) and linear units of the type $\text{M}-\text{L}-\text{M}$ ($\text{M}\cdots\text{M}$ distance ca. 3.8 Å) as present in compound **4a** (see Figure 2). Indeed, the structure determination of **4a**, as well as that of **3a** (vide infra), constitutes a rare case of a compound in which a pair of dppm ligands span a linear $\text{M}-\text{O}-\text{M}$ unit. The only previous example cited in the literature is that of the diosmium complex $\text{Os}_2(\mu\text{-O})\text{Cl}_6(\mu\text{-dppm})_2$.³⁶ The $\text{Re}-\text{O}$ terminal and bridging distances, $\text{Re}(2)-\text{O}(22)$ and $\text{Re}(2)-\text{O}(B)$, are 1.76(1) and 1.79(1) Å, respectively, and are therefore unexpectedly similar; for reference, compare with $\text{Re}-\text{O}$ distances of ca. 1.69 and ca. 1.91 Å in the structures of **3a** (vide infra) and other dirhenium(V) complexes that contain the linear $\text{O}=\text{Re}-\text{O}-\text{Re}=\text{O}$ unit.^{37,38} In contrast to the shortness of the bridge bond $\text{Re}(2)-\text{O}(B)$, the $\text{Re}-\text{O}$ distance involving $\text{Re}(1)$ (i.e. $\text{Re}(1)-\text{O}(B)$) is quite long (1.94(1) Å). The difference of ca. 0.15 Å between $\text{Re}(1)-\text{O}(B)$ and $\text{Re}(2)-\text{O}(B)$ reveals a marked asymmetry in the $\text{Re}-\text{O}-\text{Re}$ unit. It appears that a major charge disparity exists within compounds of type **4** (and presumably also in **5**), such that the $\text{Cl}-\text{Re}-\text{O}-\text{Re}=\text{O}$ unit can best be represented formally as $\text{Cl}-\text{Re}^{\text{III}}\cdots\text{O}=\text{Re}^{\text{V}}=\text{O}$ or, at least, have a major contribution from this form. Such a situation may also exist in **2**, but the direct structural evidence for this is obscured by the O/Cl disorder in the structure of **2a**. Consistent with this suggestion is our observation that the two $\text{Re}-\text{O}$ distances about $\text{Re}(2)$ in the structure of **4a** are close to those found in complexes that contain the *trans*-dioxorhenium(V) moiety (ca. 1.75 Å).^{37,39} Furthermore, the small magnetic moment measured for **4a** and the Knight-shifted NMR spectra for all complexes of type **4** and **5** presumably reflect the presence of some residual paramagnetism, perhaps localized at the "Re(III)" center. Interestingly, mono-

nuclear paramagnetic Re(III) complexes (d^4) are well-known⁴⁰⁻⁴³ to exhibit sharp, well-defined Knight-shifted ^1H NMR spectra. Temperature range magnetic susceptibility measurements on a solid sample of **4a** and on the precursor complex **2a** show that this paramagnetism is not due entirely to TIP.

When **4a-c** are oxidized by one-electron to give $[\text{Re}_2(\mu\text{-O})(\text{O})\text{Cl}_4(\mu\text{-dppm})_2(\text{CNR})]\text{PF}_6$ (**6a-c**), there is a dramatic increase in the magnetic moment (μ_{eff} ca. 3.2 μ_{B} for a solid sample of **6a**). If compounds **4** are correctly represented as approximating to mixed-valence Re(III)-Re(V) species, then it is reasonable to postulate that oxidation takes place at the more electron-rich Re(III) center. The observed magnetic moment and temperature range behavior, along with the absence of well-defined NMR spectra, are not inconsistent with the behavior expected for Re(IV).⁴⁴

The final products of the oxygenation of $\text{Re}_2\text{X}_4(\mu\text{-dppm})_2$ are the symmetric corner-sharing bioctahedral dirhenium(V) complexes $\text{Re}_2(\mu\text{-O})(\text{O})_2\text{X}_4(\mu\text{-dppm})_2$ (**3**), in which the dppm ligands maintain their bridging mode in spite of the very long $\text{Re}\cdots\text{Re}$ distances; the latter average 3.83 Å in the structurally characterized compounds **3a**· $(\text{CH}_3)_2\text{CO}$ and **3a**· CH_2Cl_2 . In both crystals, the dirhenium molecules have a crystallographically imposed center of symmetry. Like the structure of **4a**, that of **3a** is a rare example of two dppm ligands bridging a linear $\text{M}-\text{O}-\text{M}$ unit.

A comparison of the structural results for **3a** and **4a** reinforces the idea that the electronic structures of complexes of types **4** and **5** can be represented in terms of the mixed-valence form Re(III)-Re(V). The facile one-electron oxidation of **4** and **5** (and by implication of **2** also), which we have postulated occurs at the lower valent Re(III) center, accords with this being the site of the further oxygenation of **2** by O_2 to give **3**.

Acknowledgment. Support from the National Science Foundation, through Grant No. CHE91-07578 to R.A.W. and CHE89-14915 to K.R.D., is gratefully acknowledged. We also thank the National Science Foundation for Grant No. CHE86-15556, for the purchase of the microVAX II computer and diffractometer at Purdue University, and Grants CHE84-03823 and CHE89-08088 at Michigan State University, for the purchase of X-ray equipment. The Center for Fundamental Materials Research, Michigan State University, provided the funding for the purchase of the Quantum Design susceptometer.

Supplementary Material Available: Tables giving full details of the crystal data and data collection parameters for **2a**· $(\text{CH}_3)_2\text{CO}$, **3a**· $(\text{CH}_3)_2\text{CO}$, **3a**· CH_2Cl_2 , and **4a** (Tables S1-S4), atomic positional parameters (Tables S5-S10), anisotropic thermal parameters (Tables S11-S14), bond distances (Tables S15-S18), and bond angles (Tables S19-S22) and a figure showing the structure of the $\text{Re}_2(\mu\text{-O})(\text{O})_2\text{Cl}_4(\mu\text{-dppm})_2$ molecule in **3a**· CH_2Cl_2 (57 pages). Ordering information is given on any current masthead page.

- (31) Yoon, K.; Parkin, G.; Rheingold, A. L. *J. Am. Chem. Soc.* **1992**, *114*, 2210.
 (32) Cotton, F. A.; Foxman, B. M. *Inorg. Chem.* **1968**, *7*, 1784.
 (33) Lis, T. *Acta Crystallogr., Sect. B* **1975**, *31*, 1594.
 (34) Böhm, G.; Wieghardt, K.; Nuber, B.; Weiss, J. *Angew. Chem., Int. Ed. Engl.* **1990**, *29*, 787.
 (35) Böhm, G.; Wieghardt, K.; Nuber, B.; Weiss, J. *Inorg. Chem.* **1991**, *30*, 3464.
 (36) Chakravarty, A. R.; Cotton, F. A.; Schwotzer, W. *Inorg. Chem.* **1984**, *23*, 99.
 (37) Conner, K. A.; Walton, R. A. In *Comprehensive Coordination Chemistry*; Pergamon: Oxford, England, 1987; Chapter 43, pp 125-213 and references therein.
 (38) (a) Backes-Dahmann, G.; Enemark, J. H. *Inorg. Chem.* **1987**, *26*, 3960.
 (b) Basson, S. S.; Leipoldt, J. G.; Roodt, A.; Purcell, W. *Transition Met. Chem.* **1987**, *12*, 82. (c) Lumme, P. O.; Turpeinen, U.; Stasicka, Z. *Acta Crystallogr.* **1991**, *C47*, 501.
 (39) Holloway, C. E.; Melnik, M. *Rev. Inorg. Chem.* **1984**, *10*, pp 236-357 and references therein.
 (40) Randall, E. W.; Shaw, D. *J. Chem. Soc. A* **1969**, 2867 and references therein.
 (41) Gunz, H. P.; Leigh, G. J. *J. Chem. Soc. A* **1971**, 2229.
 (42) Rossi, R.; Duatti, A.; Magon, L.; Casellato, U.; Craziani, R.; Toniolo, L. *J. Chem. Soc., Dalton Trans.* **1982**, 1949.
 (43) Cameron, C. J.; Tetrick, S. M.; Walton, R. A. *Organometallics* **1984**, *3*, 240.

- (44) Figgis, B. N. *Introduction to Ligand Fields*; Interscience: New York, 1966; pp 278-279.